AD 295 410

295 410

ELECTRO-OPTICAL SYSTEMS, INC. Pasadena, California

49

Report covers 1 October - 31 December 1962
THERMAL RADIATION GUIDES FOR POWER TRANSMISSION

Prepared for

Aeronautical Systems Division
Attn: ASRMFP-3
Wright-Patterson Air Force Base, Ohio

Contract AF33(657)-8526
Project 8128, Task 61083

EOS Report 3000-Q-3 15 January 1963

Prepared by

W. J. Swenson
Project Supervisor

Approved by

D. H. McClelland, Manager
Special Projects Department

for J. Neustein, Manager
Advanced Power Systems Division

ELECTRO-OPTICAL SYSTEMS, INC., PASADENA, CALIFORNIA

The work covered by this report was accomplished under Air Force Contract AF33(657)-8526, but this report is being published and distributed prior to Air Force review. The publication of this report, therefore, does not constitute approval by the Air Force of the findings or conclusions contained herein. It is published for the exchange and stimulation of ideas.

TABLE OF CONTENTS

LIST OF ILLUSTRATIONS

LIST OF ILLUSTRATIONS (cont)

1. INTRODUCTION

This third quarterly technical progress report describes research progress directed towards achieving a fundamental advance in the state of the art of energy transmission spacecraft by a technique heretofore unexplored for this purpose. The technique herein discussed involves the transmission of radiant energy through a hollow, reflective tube from a heat source to some other location in a spacecraft without intermediate Carnot cycle limited conversion process. This technique is particularly useful for applications in which a significant portion of the total energy requirement is in the form of thermal energy. Work accomplished and reported previously has been:

1. The development of a general form of thermal radiation guide consisting of a cylindrical transmission element into which radiation energy is directed by means of a parabolic entrance "nozzle".
2. The applicability and merit of the electroforming process for the fabrication of radiation guide.
3. Use of the solar tracking facility and other test equipment on this program.
4. The basis of a detailed thermodynamic analysis.
5. Applications studies of radiation guides for lasers and thermionic power systems.
6. Hardware testing including measurements of guide efficiencies and temperatures.

Work discussed in this report includes:

1. Completion of major efforts in the thermodynamic analysis

2. The use of the thermodynamic analysis to determine a practical guide size for earth's surface testing with a conventional 5-foot diameter solar concentrator
3. A description of tooling and process details for guide fabrication
4. Preliminary testing of guide entrance to determine surface temperature effects
5. Selection of vacuum coatings for radiation guides
6. Application studies of multiple concentrators with single absorber.

2. THERMODYNAMIC RELATIONSHIP

2.1 Radiation Guide Parabolic and Cylindrical Section

The thermodynamic analysis of the parabolic and cylindrical sections of the radiation guide is performed using a difference equation technique described in the previous quarterly report, EOS 3000-Q-2. Basically, the method involves dividing the guide into differential elements, writing a heat balance equation for each element, and solving the resultant set of equations simultaneously. The heat balance equations for typical elements of the guide are described below. These results are to be used mainly as a guide to the determination of guide dimensions. For a specific system application, the results may require modification, based on empirical data. To facilitate computer solution, the notation and arrangement of the equation has been slightly modified from that which was previously reported. Using nomenclature as defined on page 33

$$KA_c \left[\left. \frac{dT}{dx} \right|_{x-\frac{\Delta x}{2}} - \left. \frac{dT}{dx} \right|_{x+\frac{\Delta x}{2}} \right] = \dot{Q}A_s - \sigma \epsilon A_s \left[T_x^4 - T_\infty^4 \right] \qquad (1)$$

where: $\dot{Q}A_s$ = Radiant energy absorbed by element

$KA_c \left[\left. \frac{dT}{dx} \right|_{x-\frac{\Delta x}{2}} - \left. \frac{dT}{dx} \right|_{x+\frac{\Delta x}{2}} \right]$ = Net heat conducted away from element

$\sigma \epsilon A_s \left(T_x^4 - T_\infty^4 \right)$ = Heat radiated from element

Convection and internal radiation (within the guide) will introduce additional terms. These are of secondary importance with respect to the steady state temperature solution and, since they introduce considerable complexity to the equations, are initially neglected. Their influence is discussed in Section 2.3 and 2.5 of this report.

The heat input values for the parabolic and cylindrical sections can be directly derived from geometrical relationships. Using the coordinates illustrated in Figure 2-1, it can be shown that:

$$\frac{I_2}{I_1} = \frac{\left(F_1/F_2\right)^2}{\left(\frac{x_2}{F_2} + 1\right)^2 \left(2 + \frac{x_2}{F_2}\right)^{1/2}}$$

$\frac{I_2}{I_1}$ = Ratio of flux density on parabolic guide surface to flux density on concentrator

The maximum flux density ratio occurs at the minimum value of x/F_2. For perfectly parallel rays of light impinging on a 60^o rim angle concentrator, the light rays reflected from the outer edge of the concentrator strike the parabolic guide at $x/F_2 = 2.0$ This value of x/F_2 is the minimum value used in the computer thermal solution. (For purposes of this analysis the focal plane rather than the vertex of the parabola is set at the origin of the coordinates.) It can be shown that the total heat absorbed by a parabolic segment of the guide is:

$$\dot{Q}_{absorber} = \alpha_2 I_2 A_s$$

$$= \frac{(\alpha_2 I_1)(F_1/F_2)^2 (\Delta x) (4\pi F_2)}{(1 + \frac{x}{F_2})^2} \quad (2)$$

Similarly, the term describing radiation away from a surface element can be expanded:

$$\dot{Q}_{radiation} = \sigma \epsilon_2 (T_x^4 - T_\infty^4) (A_s)$$

$$= (\sigma\epsilon_2)(4\pi F_2)(2 + \frac{x2}{F_2})^{1/2} (\Delta x) (T_x^4 - T_\infty^4) \quad (3)$$

The conduction term, expanded to describe the segment geometry, is:

$$\dot{Q}_{conducted} = \frac{(Kt)(4\pi F_2)(1 + \frac{x_2}{F_2})(T_{x \pm 1} - T_x)}{\left(\frac{\Delta x_n + \Delta x_{n \pm 1}}{2}\right)\left(2 + \frac{x_2}{F_2}\right)^{1/2}} \qquad (4)$$

The summation of heat transfer terms for each differential element is listed below:

Parabolic Section

$$\sum \dot{Q}_n = \alpha I_1 \left(F_1/F_2\right)^2 \frac{(4\pi F_2)(\Delta x)}{(1+\frac{x_2}{F_2})^2} + (Kt)(4\pi F_2)\frac{\frac{1+x_2}{F_2}(T_{x-1} - T_x)}{\Delta x\,(2+\frac{x_2}{F_2})^{1/2}} \qquad (5)$$

$$- \frac{(Kt)\,(4\pi F_2)(1+\frac{x_2}{F_2})(T_x - T_{x+1})}{\Delta x\,(2+\frac{x_2}{F_2})^{1/2}} - \sigma\epsilon_2(4\pi F_2)(2+\frac{x_2}{F_2})^{1/2}(\Delta x)(T_x^4 - T_\infty^4) = 0$$

Cylindrical Section

$$\dot{Q}_n = \alpha I_1 \frac{y_1^3}{y_2^2 F_1\left[1 + (\frac{y_1}{2F_1})^2\right]}(2\pi y_2)(\Delta x) + K(2\pi y_2)\frac{t}{\Delta x}(T_{x-1} - T_x)$$

$$- \frac{Kt(2\pi y_2)}{\Delta_x}(T_x - T_{x+1}) - \sigma\epsilon(2\pi y_2)(\Delta x)(T_x^4 - T_\infty^4) = 0 \qquad (6)$$

2.1.1 Method of Solution

The basic heat balance equation for each element of the guide is written using the proper input constants and element location, $(\frac{x_2}{F_2})$. Since the heat balance for each element depends on the temperature

of two adjacent elements, as well as its own temperature, the equations for the elements must be solved simultaneously. The specific technique utilized to solve the equations is known as the "Newton-Raphson Method" and is described in Ref. (1). The equations were programmed for use with the IBM 1620 digital computer, installed at EOS.

The computer program permits the use of forty differential elements, with the following input quantities variable for each element:

$$\alpha,\ \epsilon,\ \Delta x,\ K,\ t$$

In addition, the following input quantities may be varied for each case:

$$F_1,\ F_2,\ \Theta_{max.},\ D_{cylinder},\ T_\infty,\ I_1$$

2.1.2 Solution Characteristics

Since the concentrator focuses a large percentage of its collected energy on a relatively short length of guide (illustrated in Figure 2-2), considerable care in the thermal analysis must be used in correctly specifying the guide end geometry. Experience with the computer solution has shown that relatively short segment lengths ($\Delta x = F_2$) should be used for the first few segments. Beyond the first few segments, however, increased segment lengths with $\Delta x \rightarrow 10F_2$, may be used with negligible effect on the final temperature distribution.

In all solutions, the final segment is assumed perfectly insulated from the absorber; i.e., there is no conduction into or away from the "downstream" end of the final segment.

The computer solution involves an iteration procedure, with each iteration providing a correction to the individual segment temperatures. The solution is considered completed when all of the segment temperatures of a given iteration match the temperatures of the previous iteration within .05 percent $\left(\frac{T_i - T_{i-1}}{T_i} \leq .0005 \right)$. If reasonable initial guesses are made for the guide temperature, the computer normally achieves a final solution within ten iterations.

1. "Introduction to Numerical Analysis", Hildebrand, McGraw-Hill, 1959

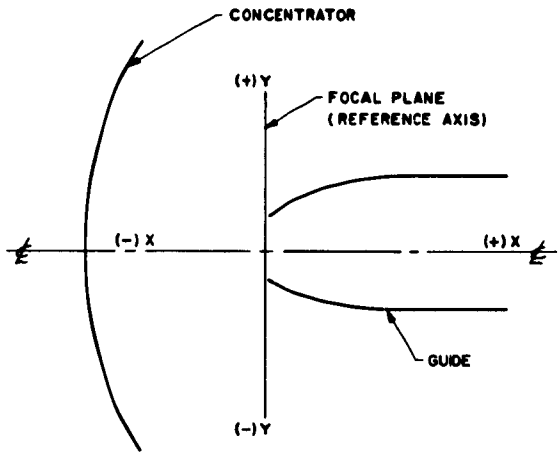

FIG. 2-1

REFERENCE AXES FOR CONCENTRATOR AND GUIDE (USED FOR EQUATIONS AND CURVES)

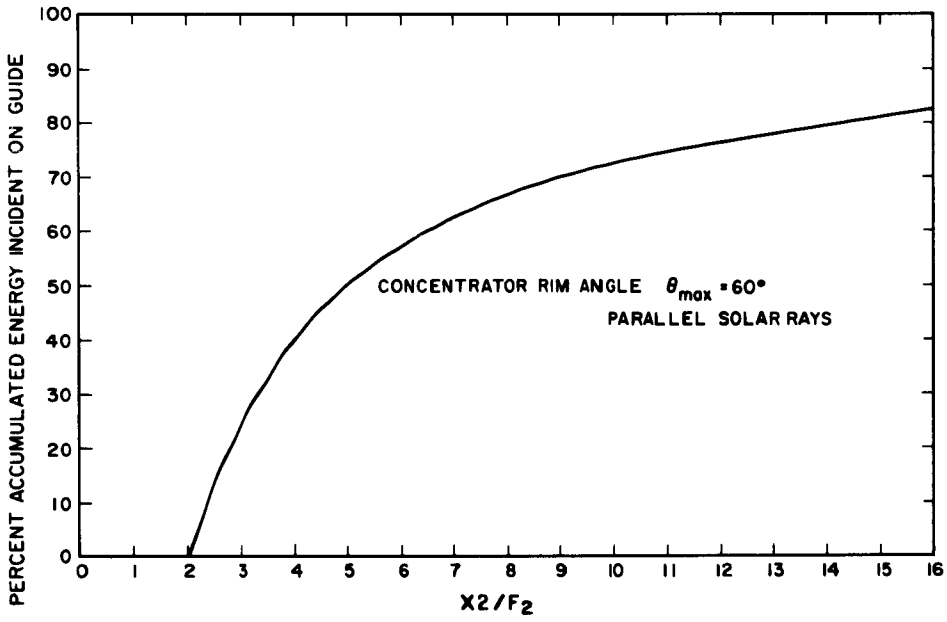

FIG. 2-2 PERCENT ACCUMULATED SOLAR ENERGY INCIDENT ON GUIDE VS AXIAL DISTANCE $\left(\frac{X_2}{F_2}\right)$ ALONG GUIDE

The difference equations used for the thermal analysis are based on the assumption of perfectly parallel light rays striking the parabolic concentrator. Although the solar angle is small ($2\gamma = 32'$), the solar image effect may be significant, particularly for large focal lengths ratios, ($F_1/F_2 \geq 200$). These effects are discussed more fully in subsection 2.2.

2.1.3 Results

Solutions to the previously described equations have been obtained for a range of input parameters considered pertinent to the design concept. The effects of the individual parameters are shown as follows:

2.1.3.1 Focal Length Ratio (F_1/F_2) - Figure 2-3

Note that the flux input density to the guide is proportional to $(F_1/F_2)^2$ and that the radiation away from the guide is proportional to T^4. If conduction effects are neglected, a thermal balance solution for each element of the parabolic guide results in:

$$T_x = \left[\frac{(I_1 \alpha)}{\left(\frac{x}{F_2} + 1\right)^2 \left(\frac{x}{F_2} + 2\right)^{1/2} (\epsilon\sigma)} \right]^{1/4} \cdot \left(\frac{F_1}{F_2}\right)^{1/2} \qquad (7)$$

Figure 2-3 indicates that, although conduction effects are significant, the relationship $T_x \sim \left(\frac{F_1}{F_2}\right)^{1/2}$ may still be used as a first order scaling factor.

2.1.3.2 Guide Conduction (K and t) - Figure 2-4 and 2-5

The influence of varying conductivities (Kt) is seen in these figures. The effect of reduced conductivity is clearly seen to increase the spread between peak and mean temperature.

2.1.3.3 Energy Absorbed by Guide (I_1 and α_2) - Figures 2-6 and 2-7

The energy input to the guide walls (proportional to I_1, α_2), without conduction effects, affects the guide temperature,

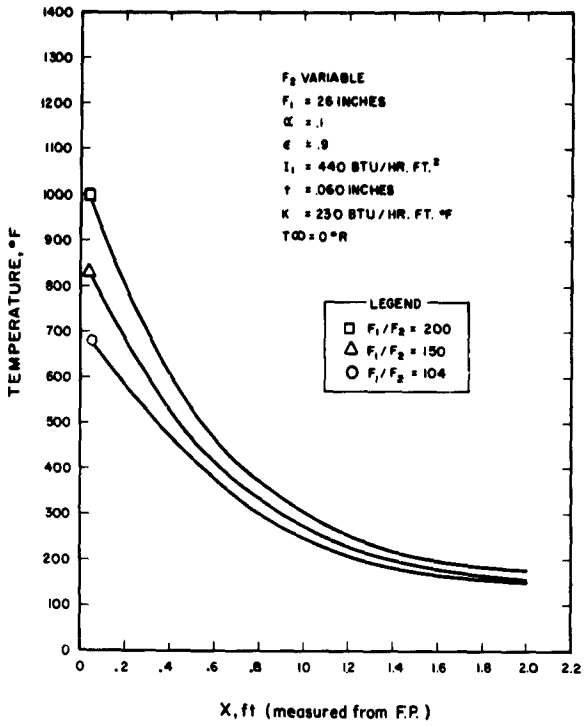

FIG. 2-3

RADIATION GUIDE TEMPERATURE VS AXIAL POSITION

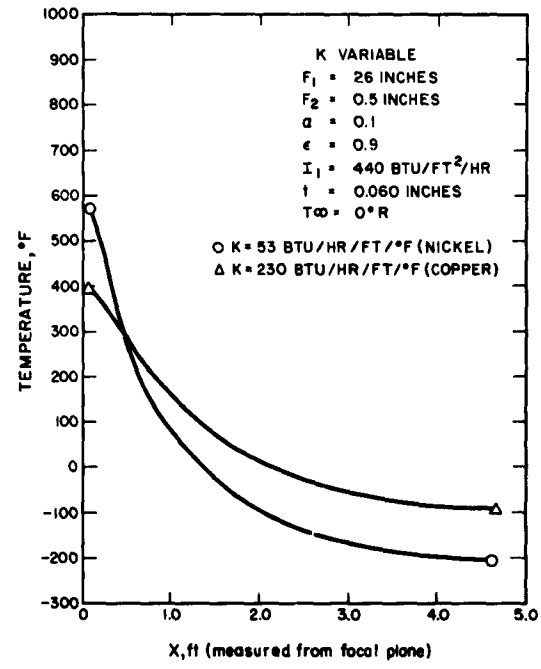

FIG. 2-4

RADIATION GUIDE TEMPERATURE VS AXIAL POSITION

T, proportional to $(I_1\alpha_2)^{1/4}$ (see Eq. 7). For the cases computed, the conduction effects tend to increase the sensitivity of temperature to input intensity slightly, although if the guide wall conductivity parameter, Kt/F_1^2, is scaled proportional to $I\alpha$, the relationship $T \sim (I_1\alpha_2)^{1/4}$ becomes a more accurate scaling factor.

2.1.3.4 Guide Length (x) - Figure 2-8

Figure 2-8 indicates clearly that additional length of guide beyond $x_2 = 100F_2$ has little influence on the peak guide temperature.

2.1.3.5 Effective Space Temperature (T_∞)-Figure 2-9

The influence of effective space temperature (T_∞), to which the guide walls radiate, is most strongly felt when guide temperatues are reasonably modest ($< 300^\circ F$). For higher guide temperatures, the effect of space temperature rapidly becomes less significant. The curve is included principally to determine correlation of ground tests with expected space environment.

2.1.4 Discussion of Results

The results presented in Figures 2-3 to 2-9 can be used to aid in the design of radiation guides for most currently anticipated uses. Although the thermal balance for each specific design can readily be evaluated, using the computer program, a few general observations can be made which may aid the designer:

1. The influence of conduction can reduce peak guide temperatures between 25 and 50 percent for reasonable wall thicknesses. Figure 2-10 presents a comparison of peak temperatures for guides of varying focal length ratios, both with and without conduction effects. The curve shown, without conduction effects, is a plot of Eq. 7, while the curve with conduction is based on computer solutions.
2. An examination of the basic difference equations indicates that the parabolic concentrator and guide dimensions may be scaled up or down, without affecting the temperature distribution of the guide if F_1/F_2 = constant, $\frac{Kt}{(F_1)^2}$ = constant.

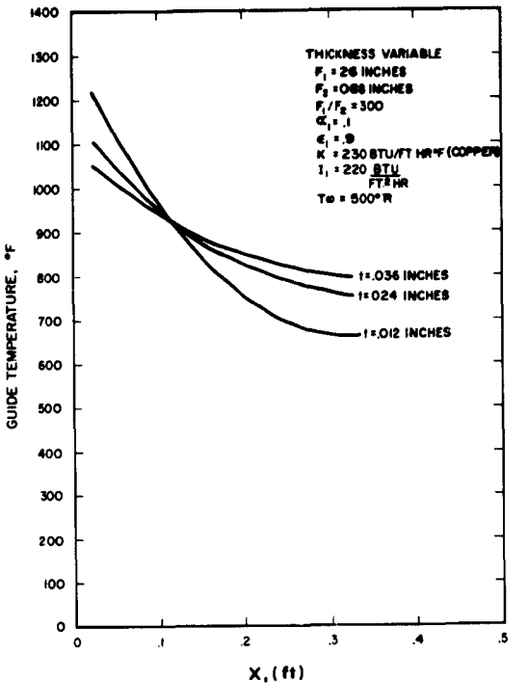

FIG. 2-5

RADIATION GUIDE TEMPERATURE VS AXIAL POSITION

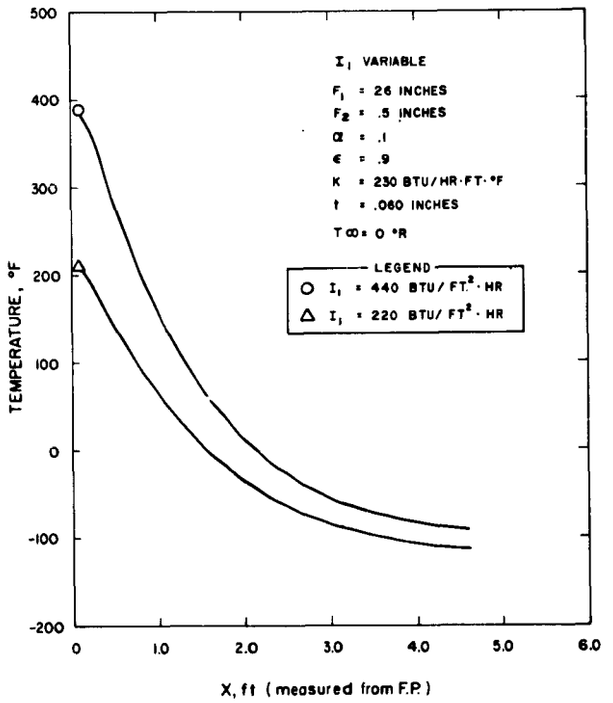

FIG. 2-6

RADIATION GUIDE TEMPERATURE VS AXIAL POSITION

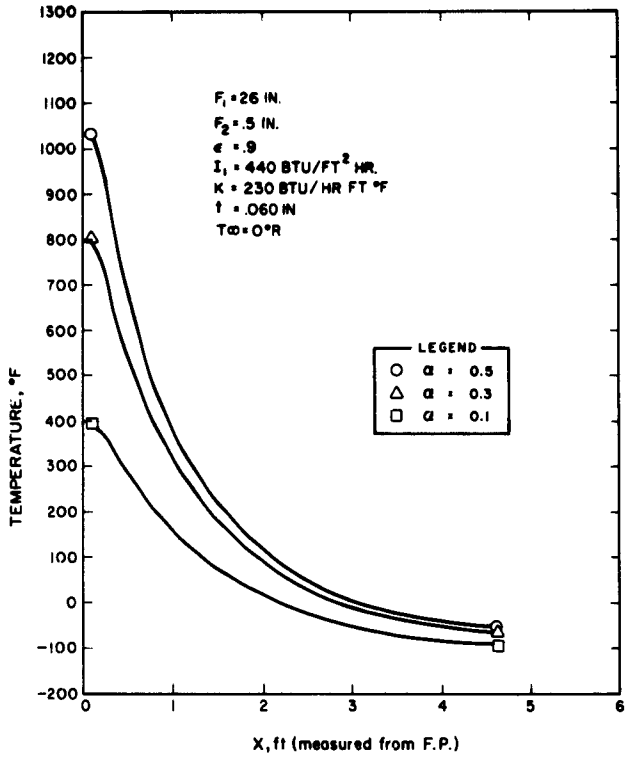

FIG. 2-7

RADIATION GUIDE TEMPERATURE VS AXIAL POSITION

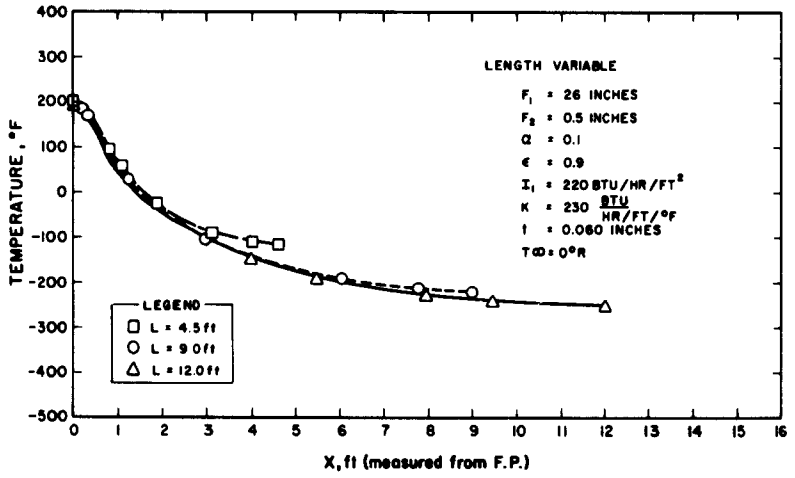

FIG. 2-8 GUIDE TEMPERATURE VS LENGTH

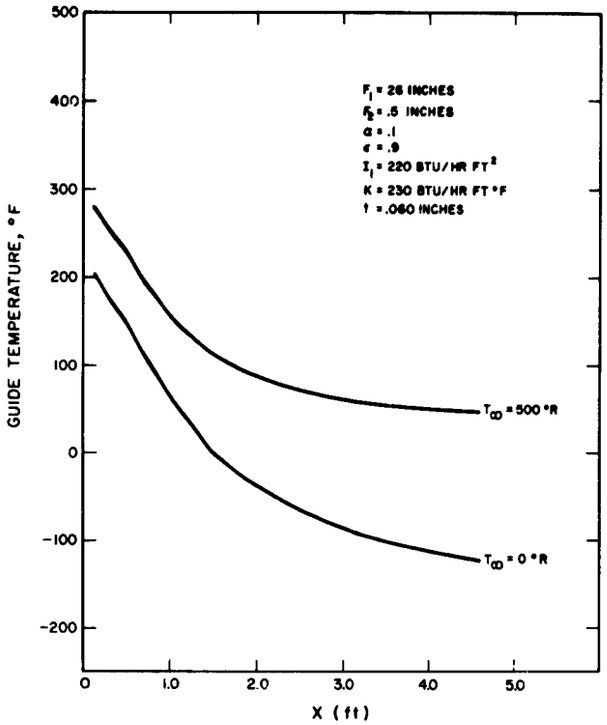

FIG. 2-9

RADIATION GUIDE TEMPERATURE VS AXIAL POSITION

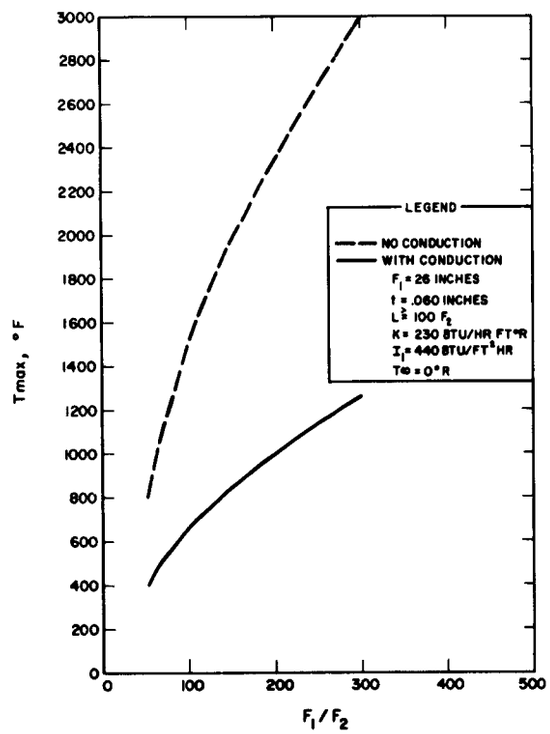

FIG. 2-10

RADIATION GUIDE MAXIMUM TEMPERATURE VS FOCAL LENGTH RATIO

These scaling factors enable guide and concentrator sizes and power levels to be scaled to any desired dimensions. Scale models can be constructed accordingly.

2.2 Effect of Solar Arc and Focal Point Coincidence

Radiant energy strikes each differential area of the parabolic concentrator with slightly converging rays, because of the finite diameter of the sun. The reflected rays are slightly diverging with the same included cone angle, as shown in Figure 2-11. A plot of the outer rays, reflected from rim surface of a 60° rim angle reflector, shown in the vicinity of the guide entrance is presented in Figure 2-12. An examination of Figure 2-12 indicates that for large focal length ratios $(F_1/F_2 \gtrsim 200)$, some of the concentrator's light energy will completely "miss" the guide entrance at the focal plane and some will impinge on its outer surface. For a finite thickness guide, some energy is also incident on the guide end. If the focal points of the concentrator and guide are not perfectly coincident, such as shown in Figure 2-12, the energy which either "misses" the guide or strikes the guide's outer surface increases with coincidence error. A plot of the total energy lost in the manner described above is shown in Figure 2-13.

The losses shown in Figure 2-13 are divided almost equally between energy missing the end of the guide and energy impinging on the guide outer surface. The energy impinging on the guide's outer surface, not only is effectively lost to the system, but may also serve to increase the temperature of the guide end. An estimate was made of the energy striking the outer surface of a guide having a focal length ratio (F_1/F_2) of 300. This additional energy was considered incident on the end segment and the resulting temperature distribution computed. The results, indicating increased guide wall temperatures are shown in Figure 2-14.

2.3 Convection Effects

The effect of convection on the steady state temperature distribution in a ground test can be included in the difference equation by the addition of the term:

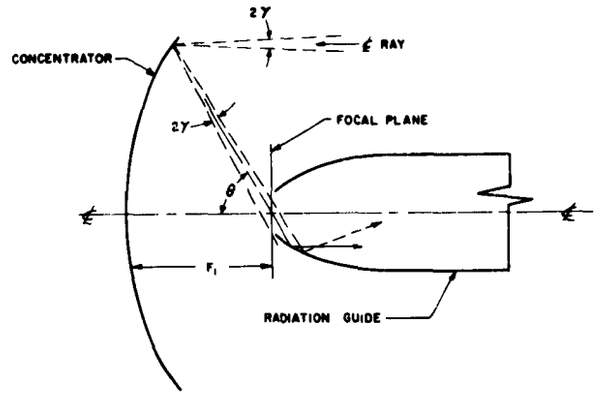

FIG. 2-11

SCHEMATIC SHOWING TYPICAL LIGHT RAY REFLECTING FROM CONCENTRATOR, IMAGING ON RADIATION GUIDE

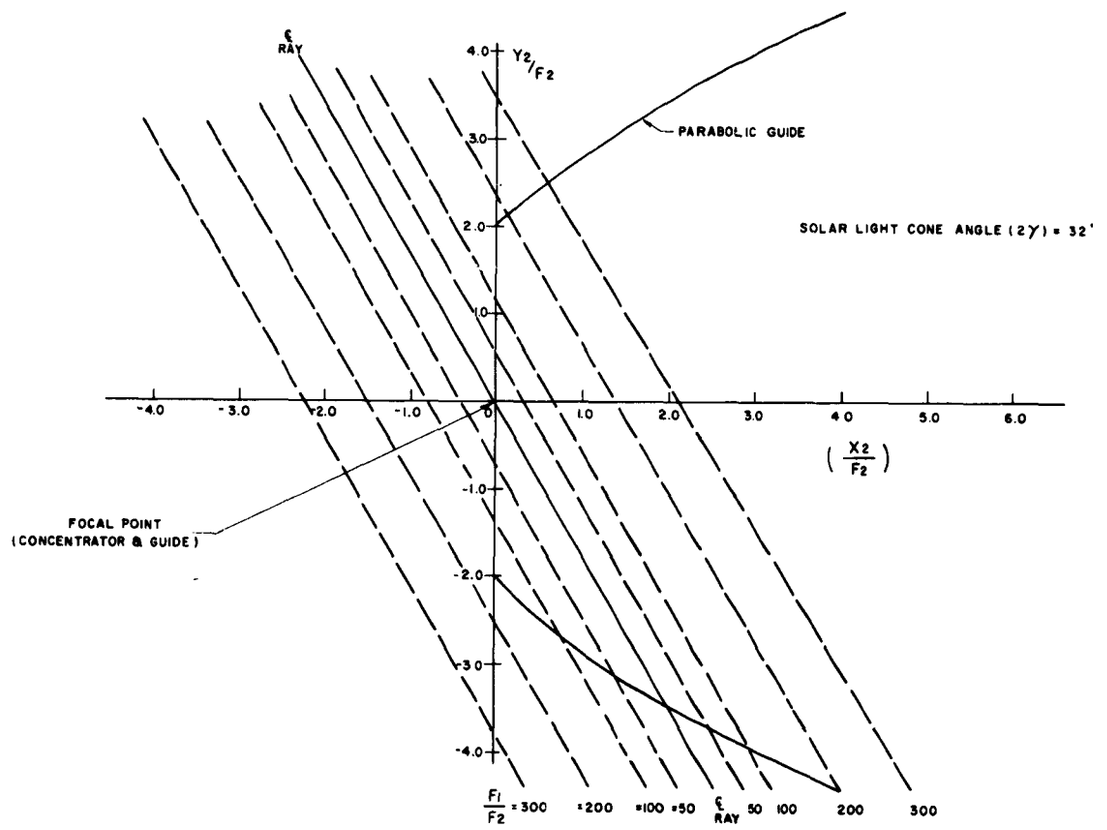

FIG. 2-12 SOLAR LIGHT RAYS FROM OUTER EDGE OF 60° PARABOLIC CONCENTRATOR

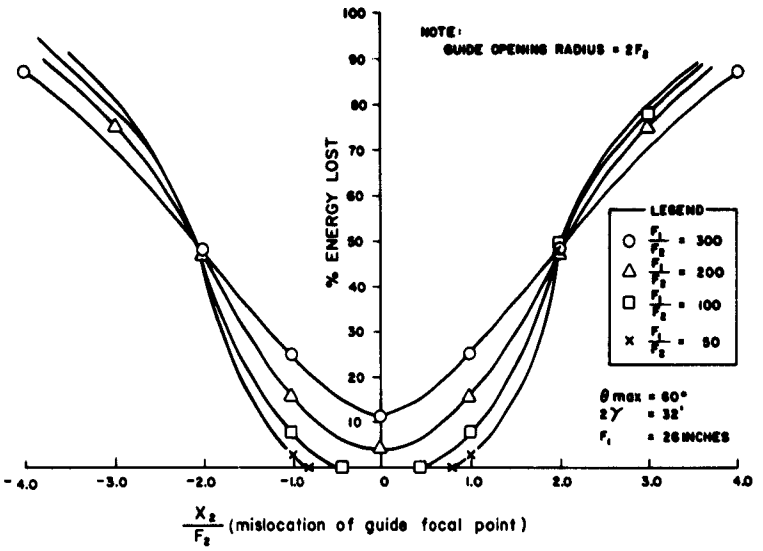

FIG. 2-13 SOLAR ENERGY LOSS VS PLACEMENT OF GUIDE ON FOCAL POINT

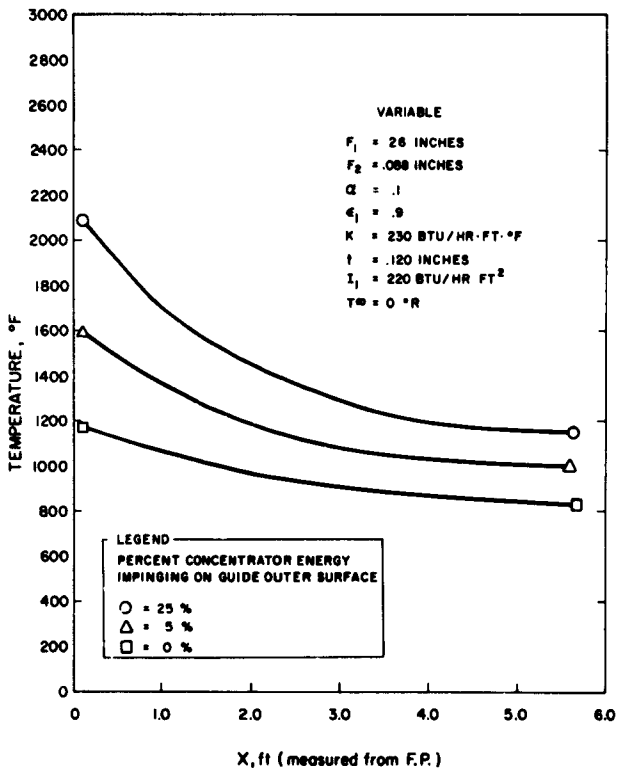

FIG. 2-14

RADIATION GUIDE TEMPERATURE VS AXIAL POSITION

$$\dot{Q}_{\text{convection}} = h_2 A_s (T - T_{\text{ambient}}) \tag{8}$$

where h_c = heat transfer coefficient

$$= \bar{c} \left(\frac{K}{L}\right)\left(\frac{g\beta\psi L^3 \rho^2 c}{\mu K}\right)^d \tag{9}$$

Since the heat transfer coefficient is a function of the properties of air, and varies with temperature, additional programming must be performed to include this term in the computer thermal analysis program. An approximation of convective effects has been made for several guide configurations. The approximation involves adjusting downward the temperature of each segment of a guide (computed without convective effects) to compensate for convective losses, while assuming that heat conducted through the element remains constant (i.e., $\frac{dT}{dx}$, remains constant). The results of this approximation is shown in Figure 2-15. For cases in which the mean temperature level of the pipe is higher than shown in Figure 2-15, convective effects become less significant.

2.4 Plane Elbow Mirror

Redirecting the light energy flowing through a radiation guide can best be performed by a plane mirror, intersecting the guide at the desired angle. An accurate analysis has not yet been made of the temperature profile across such a plane mirror surface, although a computer program can be derived to handle this case. An approximation of mirror temperature can be easily made, however, assuming uniform temperature across the mirror and no conduction away from the mirror's periphery.

Let $\dot{Q}_{3\ \text{in}} = I_1 A_1 \alpha_3$

$$\dot{Q}_{3\ \text{out}} = \sigma \epsilon_3 A_3 T_3^4$$

For thermal equilibrium:

$$I_1 A_1 \alpha_3 = \sigma \epsilon_3 A_3 T_3^4$$

$$T_3 = \left(\frac{I_1 A_1 \alpha_3}{\sigma \epsilon_3 A_3} \right)^{1/4} \qquad (10)$$

Mirror temperatures, resulting from use of Equation (10), are shown in Figure 2-16. Since conduction from the mirror's periphery will considerably reduce the mirror temperature, the values shown should be considered as conservative "upper limits".

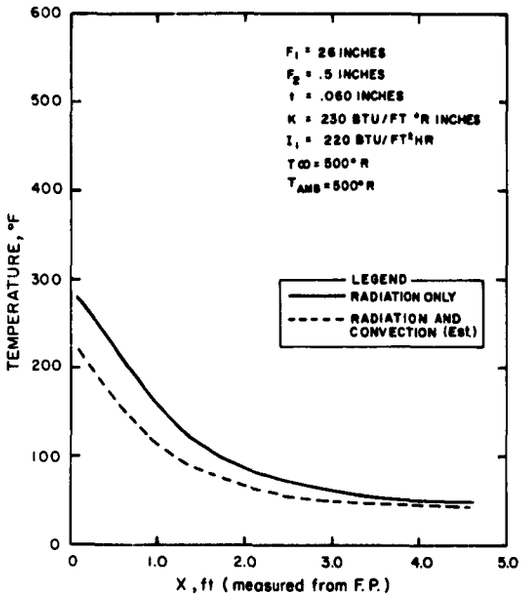

FIG. 2-15

RADIATION GUIDE TEMPERATURE VS AXIAL POSITION (convection effects simulating ground testing)

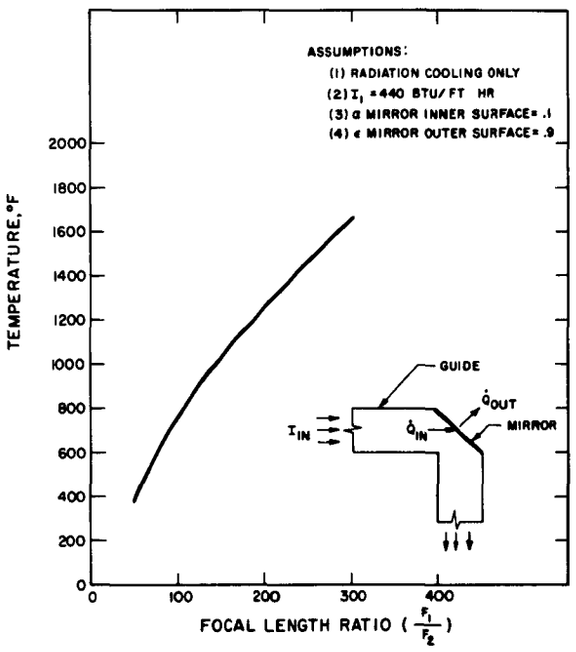

FIG. 2-16

REFLECTING MIRROR TEMPERATURE VS FOCAL LENGTH RATIO $\left(\frac{F_1}{F_2}\right)$

2.5 Internal Reradiation

The thermal analysis described previously assumes that all energy absorbed by the guide wall is eventually lost (either by radiation or convection) from the guide's outer surface. In addition, however, a transfer of energy takes place by radiation between the inner surface elements of the guide, elbow mirror and absorber.

The radiant energy leaving each element of the guide's inner surface and impinging on each other element may be readily computed (reference Quarterly Report, EOS 3000-Q-2). However, since only a small fraction of the energy incident on each element is absorbed, while the rest is specularly reflected, an involved ray tracing technique must be used to determine internal radiation energy balances for each guide temperature distribution curve. Since a large amount of work appears to be involved in ray tracing, this aspect of the problem has not yet been treated in detail. Some approximations may be made, however, and general conclusions drawn, which may help establish the potential significance of this aspect of the problem.

2.5.1 Internal Radiation - Guide Elements to other Guide Elements and to Absorber

The radiation balance will be such as to slightly reduce the guide end peak temperature and to slightly raise the guide's downstream temperature. Preliminary estimates indicate that the maximum temperature reduction will not be greater than 2 percent and may, therefore, generally be neglected in a practical design study.

Some of the internal reradiation will impinge on the absorber, thereby increasing the guide transmission system efficiency slightly over the value previously assumed $\left((\eta = (1 - \alpha)\right)$.

2.5.2 Internal Radiation - Absorber to Guide

The absorber, to which the guide supplies radiant energy, is assumed kept at a constant temperature (e.g., $T_{absorber} = 1500^{\circ}R$). The energy radiating away from the absorber impinges on

the internal surface of the guide or escapes from the guide end opening. Internal reflections from the guide's surfaces serve to redirect a considerable portion of the energy leaving the absorber back to the absorber surface, thus reducing these losses.

It is assumed that for a system consisting of a perfectly reflective thermal radiation guide coupled to a black body absorber, the entire system behaves as a black body cavity, radiating through an area equal to that of the guide opening. In order to account for the fact that the guide walls are not perfectly reflective, the area available for the escape of radiant energy is modified by the addition of the product of guide cross sectional area and guide absorptivity. These assumptions are used as a basis for preliminary analysis.

The total amount of energy lost from the absorber is assumed to be:

$$\dot{Q}_{A\ lost} \cong \sigma \epsilon_A T_A^4 \left[A_o + \alpha_2 (A_G - A_o) \right] \tag{11}$$

Using this assumption, the energy lost from the absorber may be calculated as a fraction of the total energy originally incident on the absorber. The results of these calculations, for a specific concentrator design, is shown in Figure 2-17. It should be noted that in this calculation the guide entrance is kept as a constant diameter (D = .5 in.), just sufficient to include the solar image, in order to minimize energy losses through this opening.

The effect of radiation from the absorber to the guide will generally tend to slightly increase the mean temperature of the guide. Preliminary calculations of temperature increases in the guide walls indicate that the effect is a small one and may generally be n neglected in guide design. Let

$$\dot{Q}_A \cong \sigma \epsilon_A T_A^4 A_A$$

It is assumed that the portion of $\dot{Q}_A$ absorbed by the guide is $\alpha_2 \dot{Q}_A$.

If

$T_{2\ mean}$ = mean temperature of guide neglecting radiation from absorber

$T'_{2\ mean}$ = mean temperature of guide including radiation from absorber

Then

$$(\sigma)(\epsilon_2)(\pi D_2 L_2)\left[(T'_2)^4 - (T_2)^4\right] = \alpha_2 \dot{Q}_A \qquad (12)$$

A plot of average guide temperature increase, described in Equation (12), is shown in Figure 2-18. Although the guide, in the area next to the absorber, will experience a temperature increase greater than the mean, computer calculations of temperatures at the guide entrance have shown that conduction effects limit the ratio of peak-to-average temperatures to less than 3. The resultant peak values are also sufficiently small to generally be neglected.

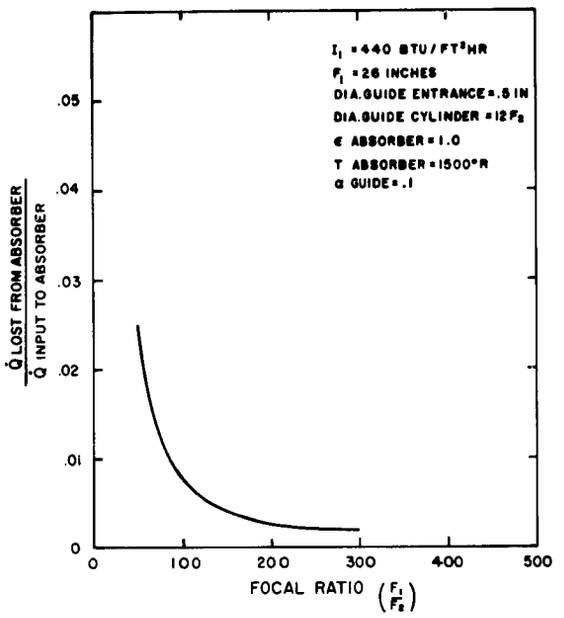

FIG. 2-17

ENERGY LOST FROM ABSORBER VS FOCAL LENGTH RATIO $\left(\frac{F_1}{F_2}\right)$

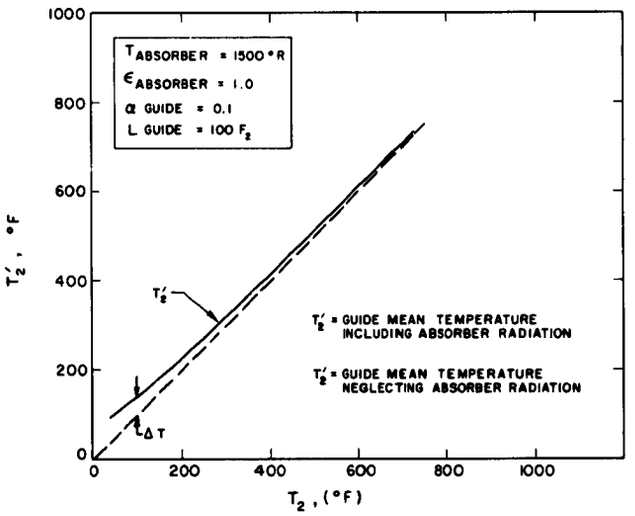

FIG. 2-18

MEAN GUIDE TEMPERATURE COMPARISON

Nomenclature

A_c - Cross-sectional area of guide surface element

A_s - Surface area of guide element

A_o - Entrance area of guide

A_G - Cross-sectional area of guide

D - Guide diameter

F - Focal length

I - Solar radiation energy density

$\dot{Q}$ - Heat transfer rate

T_x - Temperature of element, station X

T_∞ - Effective space temperature

h_c - Convection heat transfer coefficient

i - Iteration number

k - Thermal conductivity

n - Station number

t - Guide wall thickness

x - Axial position (Ref. Figure 2-1)

y - Radial position (Ref. Figure 2-1)

α - Absorptivity

ϵ - Emissivity

γ - Solar ray half angle

θ - Concentrator angle

η - Efficiency

σ - Stefan-Boltzmann constant

$(g, \beta, \psi, \rho, c, \mu)$ - Properties of air

Subscripts

1 - Refers to concentrator

2 - Refers to guide

3 - Refers to plane mirror

3. FABRICATION STUDIES

This section describes the fabrication efforts which have been followed during the last reporting period.

3.1 Guide Fabrication

As reported in Section 5 of EOS Report 3000-Q-2, it is possible to polish aluminum sheet stock so that it has a high specular reflectivity. However, further examination of this procedure has shown that polishing is undesirable from two major standpoints:

1. It is difficult to obtain consistently uniform results
2. Polishing of soft metals such as aluminum is extremely time consuming.

On the basis of the foregoing conclusions, and the good success met with electroforming at EOS, in general, it has been decided for the purposes of this project to de-emphasize the sheet metal approach outlined in EOS Report 3000-Q-2, and maintain the primary effort for fabrication of the radiation guides in the direction of electroforming.

As discussed in other sections of this report, a guide having a 6-inch diameter cylindrical section appears to be best for earth surface testing with a 5-foot solar concentrator. With this in mind, fabrication efforts have been directed towards producing a 6-inch diameter electroformed guide, fitted with an entrance parabola of 0.5-inch focal length. In order that the interior surface of the cylindrical section of the guide be accessible for surface treatments such as polishing, coating, or visual inspection, the guides will be circularly segmented as described in Section 3 and illustrated in

Figure 4-2 of EOS Report 3000-Q-2. Each segment is 24-inches long and covers 120° of arc. Each segment is provided with two paraxial flanges 0.5-inch wide, and two radial flanges, also 0.5-inches wide. A segment is illustrated in Figure 3-1. The thickness of the guide will be .060 inches, or modified on the basis of temperature experiments or refined analysis. One of the major benefits of the electroforming process for application to radiation guide, is that the thickness can be easily controlled to accommodate thermal and structural requirements.

The mandrel on which the above guide segment will be electroformed is illustrated in Figure 3-2. It is made of type 304 stainless steel, selected because of its availability, good electroforming characteristics and ability to receive and maintain a high quality optical mirror polish. The mandrel is basically a heavy-wall seamless pipe which was given a preliminary surface treatment by means of conventional grinding. To this are fitted rectangular steel bars which are the surfaces on which the integral paraxial flanges are electroformed. Attached to the ends of the tube are discs of the same material on which the integral radial flanges are electroformed. The flanges are capped with strips of acrylic plastic called "stop-offs" which make the boundary of the electroform uniform and even.

After machining and assembly the mandrel was polished by means of a 6-inch diameter cloth wheel rotating at 3750 rpm and charged with white rouge. Final hand touch-up was done by means of a suspended rouge on a cotton bag.

A suitable polish was easily obtained on the mandrel surface, thus demonstrating the validity of the decision to use the type 304 stainless steel. From these efforts, it is apparent that any degradation of the surface polishing through use and handling will be easily remedied by light repolishing operations. Additionally, it should be noted that the high hardness of type 304 stainless steel tends to minimize such degradation.

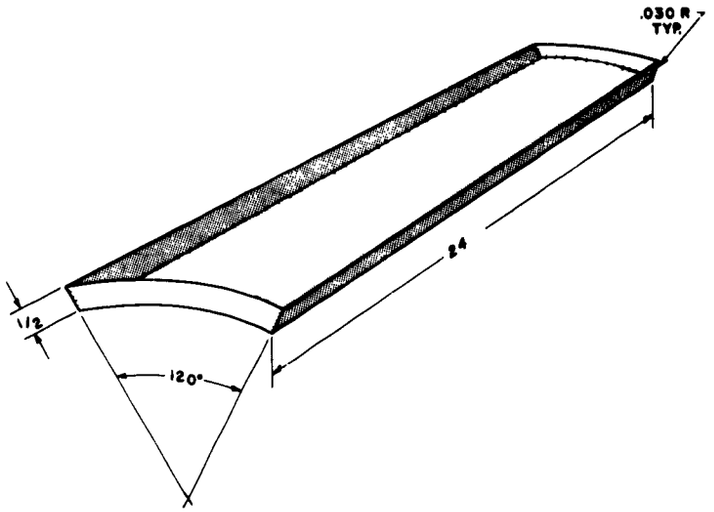

FIG. 3-1 GUIDE SEGMENT

FIG. 3-2 GUIDE SEGMENTED CYLINDRICAL MANDREL

The guide will be made of copper in order to provide the thermal conductivity necessary to assure reasonable guide wall temperature. However, copper is chemically active to many surface treatments which may be applied to the guide. To avoid this situation, the inner or mandrel side of the guide will consist of a thin skin of electroformed nickel. The mandrel will first be coated with a parting layer and then electroplated with nickel, approximately .002 of an inch thick. Copper will then be electrodeposited to the desired thickness. Previous work on the two-inch diameter guides has demonstrated the advisability of this procedure. Until it was initiated, it was difficult to remove and replace the silver reflective coating on the copper guides without destroying the electroformed surface finish of the guide itself. For the six-inch diameter guides described in this report, silver would be used only as a sensitizing and/or parting layer. When other reflective coatings or surface treatments are to be applied, it is generally necessary to remove the parting/sensitizing layer in order to assure good adherence of the reflective coating.

3.2 Spin Casting for Paraboloidal Masters

In order to generate paraboloidal masters economically, the spin casting method has been investigated. Obtainable accuracies of spin-cast masters have been adequate for the thermal radiation guide entrance section.

The spin casting method is basically this: when a liquid is rotated in a container about a vertical axis (parallel to the gravity vector) the resultant of the gravity and centrifugal force vectors will cause the liquid surface to assume the shape of the paraboloid of revolution. Thus, if a liquid were spun in this manner and could be caused to solidify while rotating, the structure of a parabolic mirror would be formed. Since this shape, however, would be a concave paraboloid, the process must be modified in order to provide a convex shape. The method which has been used on the project is to spin a

volume of mercury metal, on which is floated a solidifying plastic, such as an epoxy or polyester resin, thus generating a convex paraboloid of revolution upon solidification. The focal length, which is the primary optical characteristic of a paraboloid of revolution, is controlled by speed of rotation and by the gravity vector. For normal gravity at the earth's surface, the focal length of the paraboloid generated is given by the following formula:

$$f = \frac{17,604}{n^2}$$

where f = focal length in inches

n = speed of rotation in revolutions per minute.

While spinning and solidifying the plastic, extreme care must be taken to:

1. Eliminate vibration
2. Insure extremely constant rotating speed
3. Maintain precise verticallity of the spin axis

The first item is taken care of by using high quality spinning equipment placed on a vibration free foundation and by balancing the rotating mass.

The second item has been accomplished by employing a sensitive centrifugal governor.

Verticallity was in this case accomplished by the use of a precise machinist's level placed on the rotating body, and by careful adjustment of leveling screws under the machinery until the top of the container indicated level in all angular positions.

When all these considerations were accounted for and the conditions optimized, it was possible to produce good quality masters for electroforming purposes by this spin casting technique. A schematic picture is shown in Figure 3-3. The drive motor mechanism and bearing support assembly is a modified laboratory centrifuge. It is illustrated in Figure 3-4. Shown in this same photograph are a digital counter, which is connected to the pulse tachometer mounted on the rotor shaft;

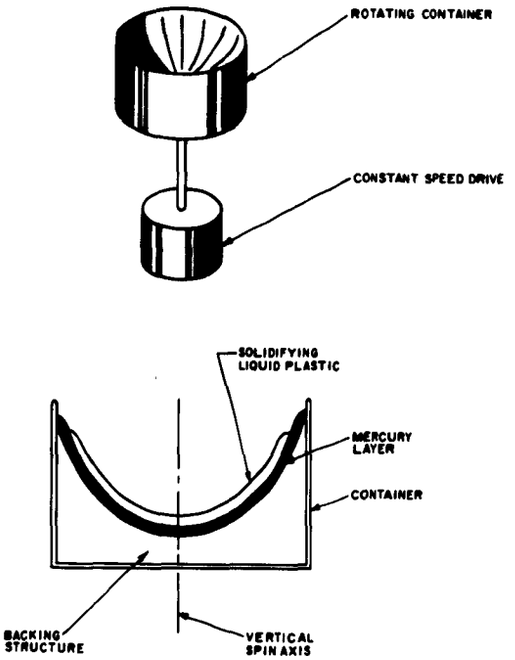

FIG. 3-3

MERCURY SPIN CASTING SYSTEM FOR THE FABRICATION OF PARABOLOIDAL MANDRELS

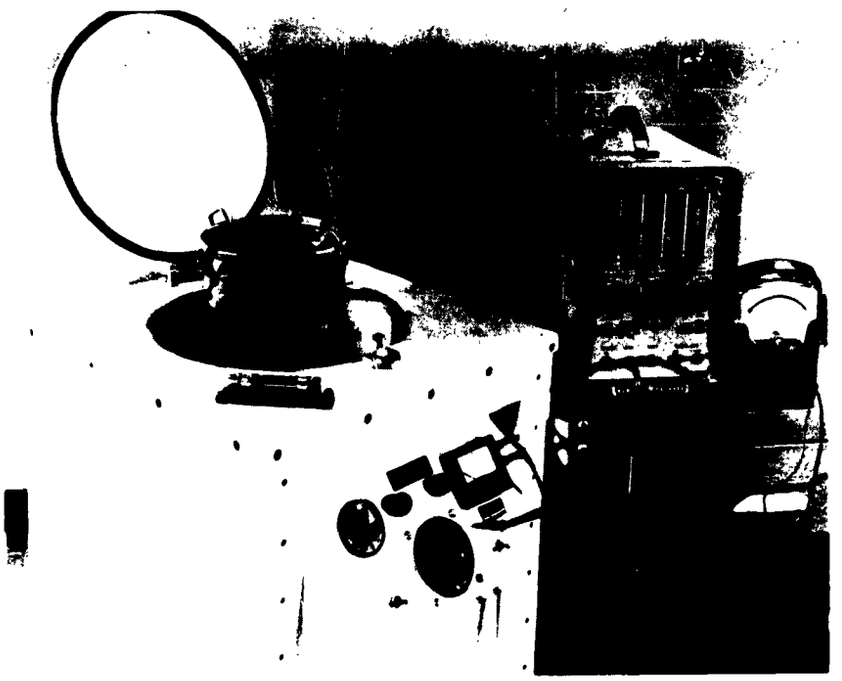

FIG. 3-4 SPIN CASTING SETUP

and a voltmeter, which indicates the satisfactory operation of the governing contacts. The amount of vibration is determined by inspection of the mercury while it is spinning. Balance adjustments are made until minimum surface ripple is evident.

Several spin-cast masters have been made by this method. Two of them are photographed in Figure 3-5. In Figure 3-6 are illustrated the electroforms which were made from these mandrels. In these particular instances, the purpose of the experiment was merely to investigate the spin casting process. However, results were sufficiently good, (determined by visual inspection of the surface, and simple optical tests) so that one of these electroforms was used in the test subsequently described in Section 5 of this report. Experimentation with various resin systems, has shown that good results can be obtained by catalyzing Shell EPON 828 with 8 phr diethylamino-propylamine. This system appears to polymerize uniformly and cure with minimum shrinkage, thus minimizing surface distortions and "wrinkles" which result when many other resin systems are used.

Primary advantage of the spin casting method is that once the equipment is set up a large variety of masters can be reproduced, varying the focal length and the diameter, at low cost per unit master. Thus experimentation is facilitated by the ready variability of such various paraboloid parameters, such as may be indicated by continuing analyses and experiments.

3.3 Coatings

Surveillance of applicable literature has not yet produced any evidence of a coating which could be considered in all respects superior to vacuum deposited aluminum. Aluminum possesses three major advances:

1. It is highly reflective, presenting a surface of 89 percent reflectivity to the solar spectrum
2. It is easily applied by means of conventional vacuum coating techniques

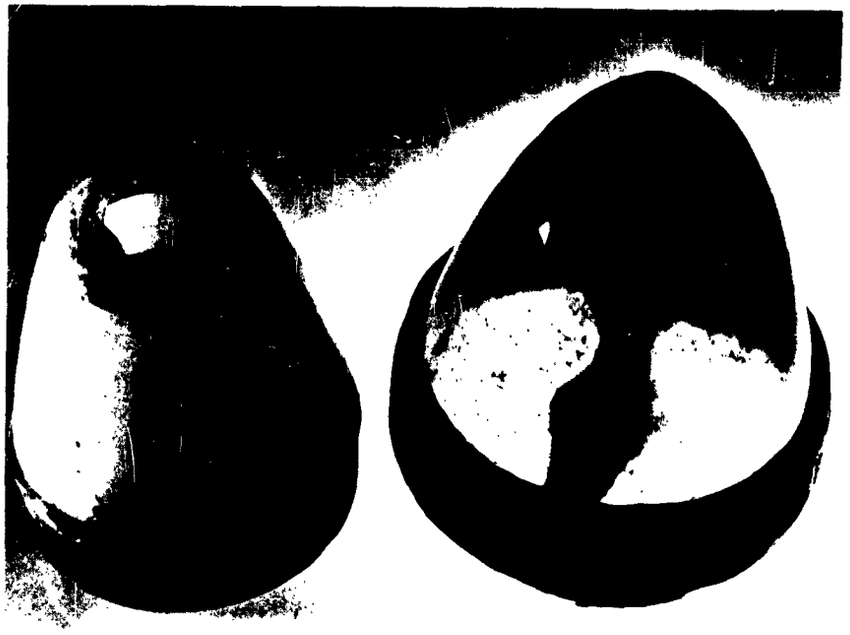

FIG. 3-5 SPIN CAST MANDRELS

FIG. 3-6 ELECTROFORMED GUIDE ENTRANCES FROM SPIN CAST MANDRELS

3. It is relatively corrosion resistant in ordinary atmospheres.

Aluminum is relatively durable at operating temperatures which would be reached in a 6-inch diameter, 1/2-inch focal length guide (with a 5-foot mirror). At these temperatures it should not tend to boil-off or sublime due to the elevated temperatures, as might be expected with a hotter guide. (Reference 2 is used as the basis of this conclusion.) The aluminum coatings can be further protected from atmospheric corrosion and possible sublimation by means of an over-coating of silicon monoxide. The silicon monoxide, vacuum deposited, is an extremely thin transparent layer which when properly applied does not alter the surface reflectivity of the substrate coating by more than 1 or 2 percent. It is naturally chemically inert and very hard. It also constitutes a dense molecular barrier which retards molecular escapes from the surface. When an aluminum coating is protected in this manner, it is found that it can be cleaned of ordinary dust and dirt, if reasonable care is used, without damage from abrasion. Silicon monoxide can be applied to aluminum with little additional difficulty. The vacuum coating machine is simply provided with an additional incandescent filament which has been submerged in a container of silicon monoxide pellets. The aluminum filaments and the silicon monoxide filament are then electrically heated in the proper sequence.

Silicon monoxide is also used with aluminum coatings as a diffusion barrier between the coating and the substrate. It has been found that for particular coating-substrate combinations, molecular diffusion takes place which generally degrades the coating. The coating molecules tend to diffuse into the substrate and vice-versa, until the coating is no longer the original material applied, with corresponding degradation of optical properties. When silicon monoxide is used as a barrier between the coatings and the substrate, molecular migration or diffusion is minimized, with resulting increase in useful coating life.

2. Jaffe, L.D., "Behavior of Materials in Space Environment," ARS Journal 32 (3) 320 (1962).

A potential problem in any vacuum coating setup is the tendency of the vaporized coating molecules to transfer along a line-of-sight path. Therefore, the filaments which have been saturated with the coating material must be arranged in such a manner that all portions of the surface to be coated are within sight of the filament. For individual elements of a segmented cylindrical guide this is not a serious problem. However, it is more difficult to coat the internal surface of a hollow cylinder (an unsegmented guide section), and attention must be given to a suitable filament array. The density of the impinging coating, may be likened to that of light flux radiating from a light source, the analogy of the filament. In order to assure uniform coating density and thickness over the entire substrate, it is necessary to have equidistant spacing between all portions of the substrate and the filaments, and to provide uniform filament temperature so that coating boil-off rate is the same along the length of the filament. A cylindrical tube can be coated with aluminum without great difficulty using a filament placed accurately along the centerline of the tube. The aluminum is applied to the filament by attaching small strips around the filament. The filament is electrically heated in vacuum to such a temperature that the aluminum melts and by capillary attraction evenly covers the entire filament. However, the silicon monoxide is not available in a form such that is can be melted and wetted to the filament. It is available only in the form of pebble-like grains, or pellets. For most coating applications these grains heated by submersing a filament in a container holding them. However, a tube can be coated by drilling the pellets and arranging them like a string of beads along the filament. An arrangement for coating hollow tubes by a wetted aluminum wire is shown in Figure 3-7. The processes for coating the inside walls of hollow cylinders have been worked out using 4-inch diameter glass tubes approximately 15 inches long. Although coatings can be applied to a hollow cylindrical tube, the coating process is difficult to control

because the filament and coated surface cannot be easily observed during coating. It is with this in mind that the cylindrically segmented guides have been developed.

The inside of the parabolic entrance section has been coated with a filament arrangement similar to that used for coating TV picture tubes. The filaments are either tapering spirals or flat-bed pans which tend to radiate uniformly over a wide solid angle.

3.4 Right-angle Bend Frame System

In order to provide something other than a straight line path of radiation transmission it is a necessary part of this project that a method of bending the radiant flux path be devised. Conceptually, this can be done by placing a plane mirror in the flux transmission path so that the flux is reflected from the plane mirror and thus oriented differently from the original direction. Arrangements of this nature were described in Sections 4.2 and 4.1.1, and illustrated in Figures 8 and 13 of EOS Report 3000-Q-2. During this last reporting period the detailed design of a right angle framework has been made. This system is a fixed bend, and does not incorporate any flexible joining techniques. As illustrated in Figure 3-8 it consists of an aluminum framework into which two guide cylinder segments and a plane mirror are fitted. The framework is made of aluminum in order that it may be kept light in weight for future space applications and also for convenience in support during ground testing. The guide cylinder segments can be made from the angularly segmented guides as described in Section 3.1 of this report. They would, of course, have to be cut at the proper 45^{o} angle for mounting into the right angle bend framework. Inasmuch as Section 2 of this report emphasizes the necessity of thermal conductivity along the guide walls to maintain low guide temperatures, it is important that maximum thermal conductivity through the right angle bend framework be maintained, especially if the bend is near the paraboloid. It is anticipated that the guide segments will be soldered to the right angle bend framework, thus providing maximum

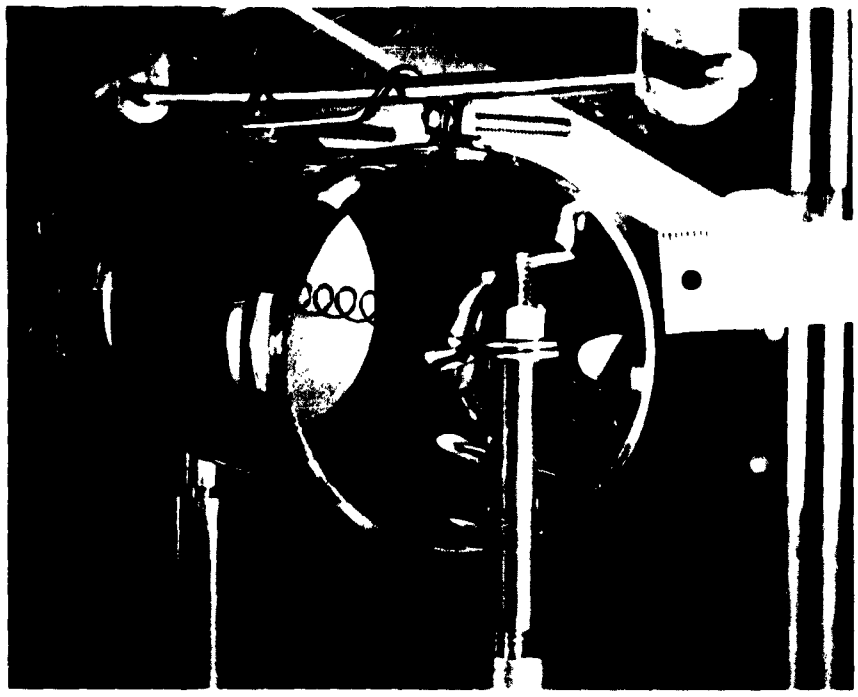

FIG. 3-7 COATING FILAMENT ARRANGEMENT FOR HOLLOW TUBES

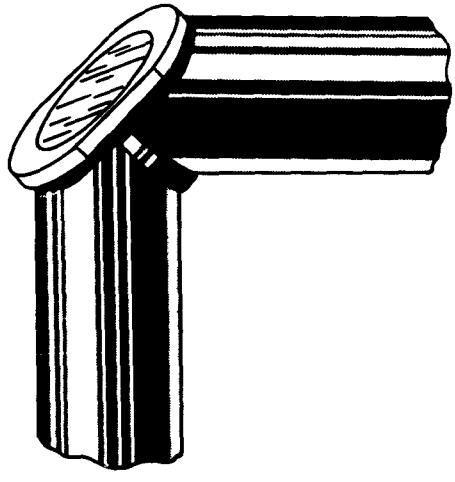

FIG. 3-8 RIGHT ANGLE FRAME

contact area. In order to facilitate soldering, the framework will be electroplated with a solderable coating, such as gold, copper, or silver. The plane mirror, as currently conceived, would be screw-mounted to facilitate removal, and replacement for experimental purposes. If necessary to improve thermal conductivity, the plane mirror could be soldered to the framework. However, the thermodynamic analysis indicates that even with no cooling by conduction to the framework, the plane mirror will operate at sufficiently low temperatures. Even these temperatures are conservatively high, because some conductive cooling will be present due to the metal-to-metal contact between mirror and framework. This framework is now being built.

4. APPLICATIONS

The application discussed in this section is the use of the thermal radiation guide to provide thermal coupling from a multiple array of solar concentrators to a single absorber. This configuration obliterates the need for a single large concentrator. All other things being equal a single large unit is better than many small units. However, it may be desirable use several smaller concentrators rather than a single large concentrator for the following reasons:

1. Ship board storage and launch package volume is decreased. This same advantage is true of large petal type collapsible concentrators. However, the small one-piece mirrors can be made more accurately than a large petal mirror.
2. 60-inch diameter, 26-inch focal length solar concentrators are readily available, and generally do not require new tooling. A large concentrator encompassing the same areas as a number of 60-inch concentrators, would require new tooling and a rather large investment.

A typical arrangement is illustrated in Figure 4-1. Here the solar energy impinging on four solar concentrators is eventually directed into the single absorber.

The main concept which must be developed for this particular application is the configuration of the junction of the four radiation guides. This could be accomplished by providing the absorber with a hemispherical reflective front cover piereed with four holes through which the radiation guides enter. The reflective cover serves to

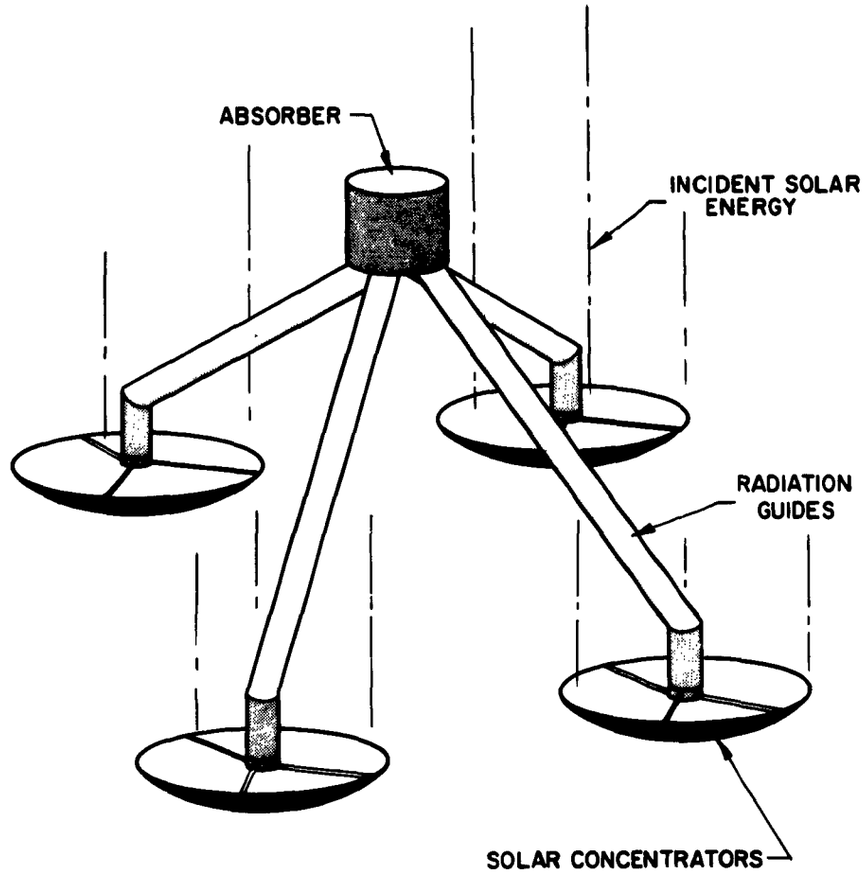

FIG. 4-1 MULTIPLE CONCENTRATOR ARRANGEMENT

retain the energy delivered to the absorber by preventing its reradiation except through the guide entrance orifices. Another possible guide coupling configuration could be developed geometrically by the sectioning of the individual guides as they approach the intersection for centerlines, such that no guide would interfere with the flux path of any other guide. This latter concept has the advantage that a smaller reflective surface is presented to the absorber radiation, and less energy is lost due to the imperfect reflectivity of the reflective cover. In the reflective cover scheme it is possible that enough energy would be absorbed by the cover to cause its destruction unless auxiliary cooling was provided.

The construction and testing of a full-scale system would be outside the scope of this project. However, the scale factors developed in Section 2. of this report show that a scale model could be designed, constructed, and tested in such a manner that the results could be extrapolated to a full-scale version.

5. TESTING

During this past reporting period, hardware testing has been de-emphasized, until a good configuration could be developed. During this reporting period, the thermodynamic analysis (see Section 2) has indicated a suitable configuration and set of guide dimensions for a thermal radiation guide which should operate at reasonable temperatures during solar testing. Fabrication efforts currently underway and expected to be completed shortly will be the basis for complete and highly significant solar and nuclear testing. However, one test made during this last reporting period verifies the validity of the thermodynamic analysis.

5.1 Test Equipment

As a result of the apparent necessity of constructing guides of at least six inches diameter, a water calorimeter which will accommodate guides of this size has been designed and built. This calorimeter consist of an absorber disc made of a flat coil of copper tubing through which water is ducted. The absorber side of the disc is blackened so that its absorptance is nearly 100 percent. The opposite side is thermally insulated with a polyester foam in order to minimize extraneous heat fluxes which would invalidate the calorimetric measurements. This calorimeter is in other respects similar to that described in Section 5.1.2.1 and illustrated in Figure 16 of EOS Report 3000-Q-2. The test setup in which the calorimeter would be included is identical to that described in the same sections of EOS Report 3000-Q-2. This calorimeter can be adapted for hot-calorimeter studies by placing an isolated absorber disc of a refractory material in front of the present absorber disc.

Energy entering the hot calorimeter will first impinge on the refractory absorber which will reach its equilibrium temperature and then reradiate onto the water cooled copper coil. Regulating reflectors will be inserted between the cooling coil and the refractory absorber in order to control the temperature of the hot absorber disc. In this manner the thermal radiation path between the absorber and cooling coils will be variable so that the absorber temperature can be maintained at any desired level up to the maximum heating capability of the guide. A small peep-hole is provided in the back of the calorimeter so that the hot absorber temperature may be monitored by an optical pyrometer. The 6-inch calorimeter is schematically and photographically illustrated in Figure 5-1. The hot calorimeter is schematically illustrated in Figure 5-2.

5.2 Temperature Testing of 6-Inch Diameter 1/2-Inch Focal Length

In order to bear out the conclusions of the thermodynamic analysis the paraboloid described in Section 3.2 of this report was tested for surface temperature. Since, at the time of the testing, the cylindrical guide was not available, it was necessary to simulate the heat sink affect which would have been provided by such a cylindrical guide section. To accomplish this, a water cooled rim was fitted to the parabola. The water cooled rim was operated at a temperature of $92^{\circ}F$. The test setup is photographed and schematically illustrated in Figure 5-3. The guide temperature as measured on the external surface was found to be less than $150^{\circ}F$. Inasmuch as this was only a partial test, colored temperature-sensitive paints, rather than thermocouples, were used as a temperature measuring medium. As an incidental measurement, guide efficiency was also computed. It was found to be in the neighborhood of 70 percent.

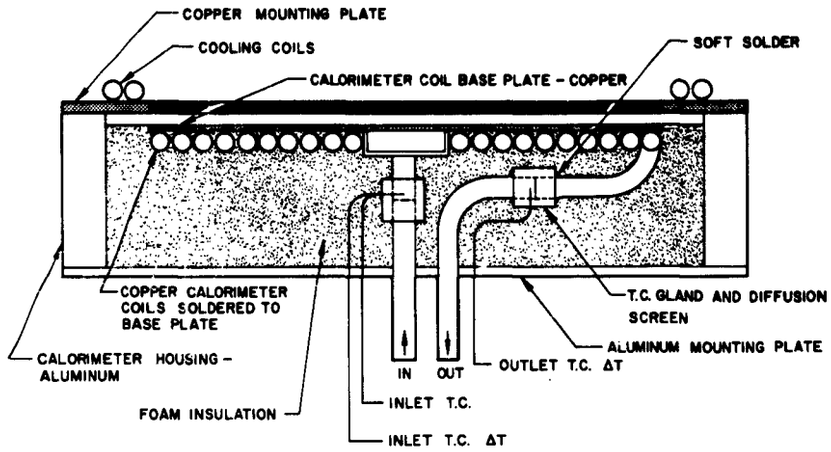

FIG. 5-1 SIX INCH CALORIMETER

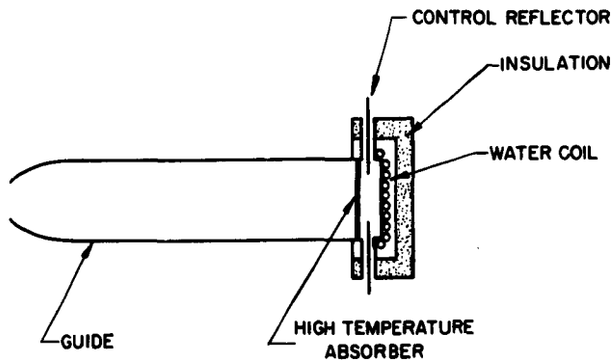

FIG. 5-2
HOT SIX INCH CALORIMETER

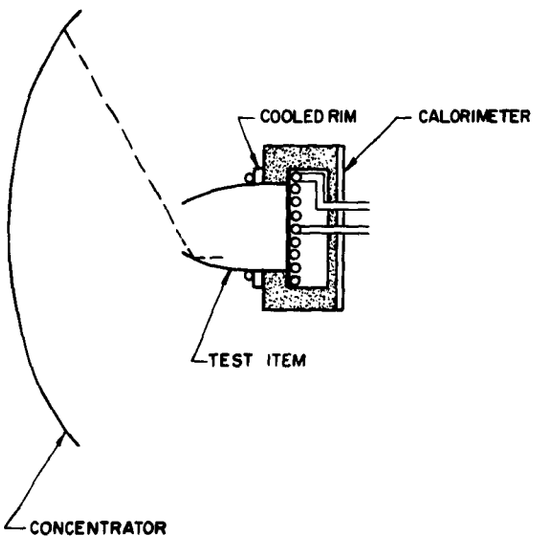

FIG. 5-3

TEST SETUP OF 0.5 INCH FOCAL LENGTH GUIDE PARABOLOID

5.3 Reradiation Testing

The thermodynamic analysis, Section 2 of this report, has shown that it is extremely difficult, within the scope of this project, to calculate with any precision the reradiation energy from the absorber coupled to the radiation guide. It is apparent then that the major effort in this direction must be made experimentally. With this in mind, the test will be made using a guide in which the absorber is replaced by an electric heater operating at various temperatures in order to simulate a high temperature absorber. For this testing, a 2-inch diameter guide, 26-inches long, fitted with a parabolic entrance, focal length of .088 inches will be provided with an electric heater, The test setup is illustrated in Figure 5-4. As illustrated a standard calorimeter will be provided adjacent to the guide entrance, thus receiving all radiant energy exiting from this orifice. The electric heater coupled to the "downstream" end of the guide will recive its energy through a wattmeter in order to determine the amount of power entering the guide. The electric power can be controlled by means of a rheostat or variable power supply. The system is provided with a peep-hole so that the heater surface temperature, simulating the absorber temperature, may be monitored. The back side of the heater is provided with a water cooling jacket, which in turn is insulated from the environment, in order that the total amount of heat collected in the guide, the calorimeter, and the water jacket, may be known and thus the accuracy of the experiment verified.

The most important results expected to be gain from this experiment are the amount of radiation loss through the guide orifice, and the amount of energy absorbed on the guide walls. The latter may in some cases be partially recovered. It also affects the guide wall temperatures. This experiment is now underway and results will be reported at a later time. The heater surface temperature is monitored as described above and in this experiment will be varied at suitable

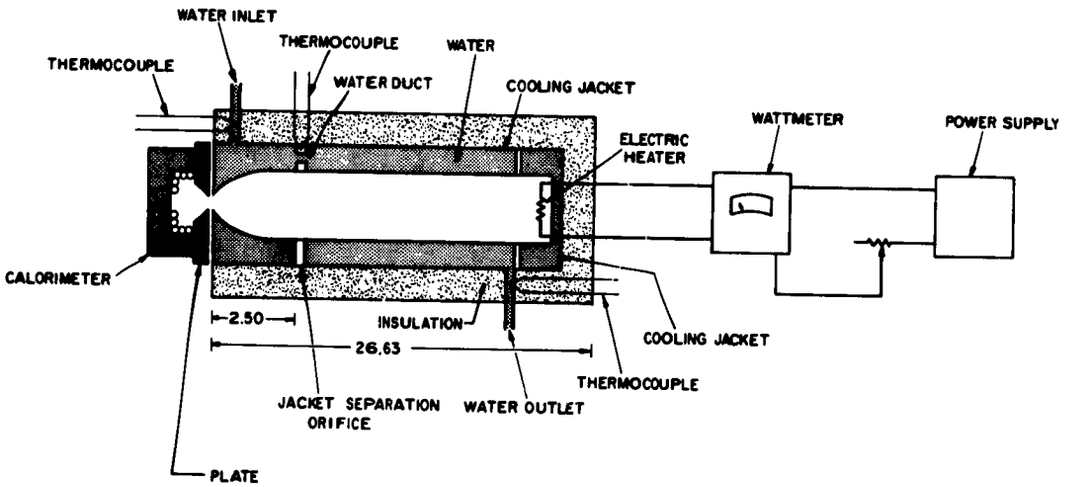

FIG. 5-4 RERADIATION TEST SETUP

intervals from 500 to 1500°F. Attempts will be made to vary the reflectivity, or absorptivity, of the guide coatings in an effort to determine the effect of this variation on the guide wall temperatures and on the quantity of reradiated energy. An uncooled guide may be tested in a similar manner, in an effort to determine the effect of guide wall temperatures on transmission efficiency, due to the radiation of the guide walls themselves.

5.4 Multiple Concentrators Testing

One of the most interesting potential applications of the thermal radiation guide is to enable the collection of energy from a number of solar concentrators and deliver it to a single absorber. For ground testing a setup of this nature would be prohibitively expensive and clumsy when applied to the normal 5-foot diameter concentrators. However, when the dimensionless parameters as discussed in the thermodynamic analysis, Section 2 of this report, are considered, it is evident that it is possible to test a scale model of such a multiple concentrator system. The important things to keep consistent are the focal length ratio, (concentrator focal length divided by guide paraboloid focal length) and the thickness coefficient to t/F_1^2. With this in mind, it is proposed to make additional use of the two-inch diameter, .088-inch focal length guides previously developed and constructed on this project. Using these guides, and the consistency of the dimensionless parameters, a model could be made which would employ 10.6 diameter 4.6-inch focal length reflectors in the place of the 5-foot diameter solar concentrators. Reflectors fitting this description precisely are not readily available. However, a satisfactory approximation can be made by using the easily obtainable 12-inch diameter, 5-inch focal length mirrors. A system of this nature, employing 4 concentrators, is illustrated schematically in Figure 4-1. A complete system of this type would be of size and weight which could easily be mounted and operated in the modified searchlight type solar tracker. This system is still in the preliminary stage of planning.

6. FUTURE EFFORTS

During the next monthly reporting period, progress will be directed along the following lines:

1. Refinement of the thermodynamic equations as may be necessary
2. Completion of the fabrication of the 6-inch diameter guide as discussed in this report
3. Testing of the guide for efficiency and temperature
4. Continuation of the application study
5. Design of a multiple concentrator scale model.